Published in final edited form as:
Clin Cancer Res. 2009 August 1; 15(15): 4993–5001. doi:10.1158/1078-0432.CCR-08-2222.

DCE-MRI as a predictor of clinical outcome in canine spontaneous soft-tissue sarcomas treated with thermoradiotherapy

BL Viglianti[1,2], **M Lora-Michiels**[1,5], **JM Poulson**[2,7], **Lan Lan**[3], **D Yu**[3], **L Sanders**[3], **O Craciunescu**[2], **Z Vujaskovic**[2], **DE Thrall**[6], **J MacFall**[4], **HC Charles**[4], **T Wong**[4], and **MW Dewhirst**[2,*]

[2]Departments of Radiation Oncology, Duke University Medical Center, Durham, NC 27710

[3]Biostatistics and Bioinformatics, Duke University Medical Center, Durham, NC 27710

[4]Department of Radiology, Duke University Medical Center, Durham, NC 27710

[6]School of Veterinary Medicine, North Carolina State University, Raleigh NC 27695

Abstract

Purpose—This study tests whether DCE-MRI parameters obtained from canine patients with soft tissue sarcomas, treated with hyperthermia and radiotherapy, are predictive of therapeutic outcome.

Experimental Design—37 dogs with soft tissue sarcomas had DCE-MRI performed prior to and following the first hyperthermia. Signal enhancement for tumor and reference muscle were fitted empirically, yielding a washin/washout rate for the contrast agent, tumor AUC calculated from 0 to 60s, 90s, and the time of maximal enhancement in the reference muscle. These parameters were then compared to local tumor control, metastasis free survival, and overall survival.

Results—Pre-therapy rate of contrast agent washout was positively predictive of improved overall survival and metastasis free survival with hazard ratio of 0.67 ($p = 0.015$) and 0.68 ($p = 0.012$) respectively. After the first hyperthermia washin rate, AUC60, AUC90, and AUCt-max, were predictive of improved overall survivaloverall survival and metastasis free survival with hazard ratio ranging from 0.46 to 0.53 ($p < 0.002$) and 0.44 to 0.55 ($p < 0.004$), respectively. DCE-MRI parameters were compared with extracellular pH and 31-P-MR spectroscopy results (previously published) in the same patients demonstrating a correlation. This suggested that an increase in perfusion after therapy was effective in eliminating excess acid from the tumor.

Conclusions—This study demonstrates that DCE-MRI has utility predicting overall survivaloverall survival and metastasis free survival in canine patients with soft tissue sarcomas. To our knowledge, this is the first time that DCE-MRI parameters have been shown to be predictive of clinical outcome for soft tissue sarcomas.

*Corresponding Author: Mark W. Dewhirst, DVM, PhD, Department of Radiation Oncology, Box 3455, Duke University Medical Center, Durham, NC 27710, dewhi001@mc.duke.edu phone: 919-684-4180, fax: 919-684-8718.
[1]Both authors contributed equally
[5]Current Address: School of Veterinary Medicine, Tufts University, North Grafton, MA 01536
[7]Current address: School of Veterinary Medicine, Purdue University, West Lafayette, IN 47907

Clinical Relevance:
This study demonstrates the ability to predict overall survival and metastasis free survival of canine patients with soft tissue sarcomas using MRI prior to and 24 hrs after the neoadjuvant hyperthermia/radiation therapy. In soft tissue sarcomas early metastasis is a common problem, requiring aggressive neo adjuvant, surgery, and adjuvant therapy in order to have a favorable outcome. The ability to use DCE-MRI to stratify these patients would have significant clinical impact in its subsequent potential to influence the aggressiveness of neo/adjuvant therapy along with determining if the therapy will be an effective treatment. To our knowledge this is the first study to demonstrate the use of DCE-MRI in soft tissue sarcomas and have an independent predictive ability on treatment efficacy.

Keywords

DCE-MRI; washin; AUC; Hyperthermia; canine; hypoxia; reoxygenation; soft tissue sarcoma

Introduction

Numerous Phase III clinical trials have demonstrated that thermoradiotherapy is superior to radiotherapy alone for achieving local tumor control and in some cases, improving survival. (1,2,3,4,5,6) It is well known that hyperthermia changes tumor oxygenation, inhibits DNA damage repair, and is directly cytotoxic. (7,8) The effects described above are strongly dependent on temperature and duration of heat exposure but which effect dominates in improving tumor control with thermoradiotherapy is not known. In pre-clinical models, mild to moderate heating (41–43°C) leads to increased perfusion and oxygenation, whereas higher thermal exposures can cause vascular damage and hypoxia. (8) Presumably, this latter effect would be deleterious to optimal thermoradiotherapy response, but there are no definitive clinical studies demonstrating this.

Previous work with canine sarcomas have reported improved oxygenation following a single hyperthermia treatment when median temperatures were less than 44°C (9) and that changes in oxygenation can persist throughout a course of fractionated thermoradiotherapy. (10) Panjapour et al. reported that perfusion was improved throughout a course of thermoradiotherapy in dogs with mast cell tumors. (11) These data support the notion that part of the effect that mild hyperthermia has in improving radiotherapy response is due to increased oxygenation through improved perfusion. However, in neither of these reports was there a correlation made between changes in pO2 or perfusion and treatment outcome.

Brizel et al. reported that improvements in oxygenation 24 hr after the first hyperthermia treatment were associated with higher pathologic complete response rates after thermoradiotherapy of human soft tissue sarcomas. (12) Jones et al. presented similar data in a small series of 13 patients with locally advanced breast cancer who were treated with a combination of hyperthermia, paclitaxel and radiotherapy. (13) The response endpoints reported in both of these studies were relevant to short term cell killing, but neither addressed the more important issue of the effects of reoxygenation on local tumor control.

Because of the importance of perfusion in cancer therapy (with or without hyperthermia), Dynamic Contrast Enhanced-MRI (DCE-MRI) has been gaining use to obtain physiological information. This imaging method provides information related to perfusion and permeability-surface to volume product of a region/voxel of interest.

Recently we reported results from a randomized phase II clinical trial involving thermoradiotherapy treatment of canine soft-tissue sarcomas. (3) Results of this trial indicated that higher thermal dose was associated with significant prolongation of progression free survival. Extracellular pH and 31-P MRS parameters were associated with metastasis free and overall survival in a subset of patients from this same trial. (14) In this particular study we evaluate the potential of DCE-MRI derived parameters, obtained before treatment and 24 to 72 hours post first hyperthermia treatment, to be prognostically predictive in subset of 37 patients who were evaluated with MRI as part of this trial.

Materials and Methods

Patients and Clinical Trial Design

Thirty-seven canine patients with spontaneously-occurring soft tissue sarcomas were randomized to receive either a low (2–5) or high (20–50) thermal dose quantified as cumulative equivalent minutes that the T90 was equal to 43°C (CEM43°CT90), in combination with fractionated radiotherapy (56.25Gy in 25 daily fractions of 2.25Gy). T90 refers to the temperature reached or exceeded by 90% of measured temperature points. Tumor types included 20 hemangiopericytomas (54.1%), 9 fibrosarcomas (24.3%), 4 myxosarcomas (10.8%), 2 neurofibrosarcomas (5.4%), and 2 non-specific sarcomas (5.4%). Classification of histologic subtype was performed by a board certified veterinary pathologist. (15) Hyperthermia was induced using microwave applicators operating between 140 and 433 MHz. Thermal dose randomization was stratified by tumor volume and tumor grade. Approximately one hyperthermia treatment was given per week, after the daily radiation fraction. The duration of the hyperthermia treatment was adjusted so as to administer approximately 20% of the prescribed hyperthermia total dose in each hyperthermia fraction. Occasionally the prescribed thermal dose was administered in 4 weekly treatments, and in some other dogs, a 6^{th} treatment had to be added to reach the prescribed thermal dose (3) Magnetic resonance imaging was performed before and 24–72 hours after the first hyperthermia treatment (Figure 1).

The procedures were approved by the North Carolina State and Duke University Animal Care and Use Committees.

Dynamic Contrast-Enhanced Magnetic Resonance Image Acquisition

All studies were performed on a GE 1.5T Signa System equipped with a surface coil. Dogs were anesthetized with isoflurane (Abbott Laboratories, N Chicago, IL) for the MR study. Coronal and axial localizer images (fast spoiled gradient recalled echo pulse sequence) were acquired initially to define tumor position. Five baseline scans consisting of fifteen T1-weighted images (TR = 400, TE = 15) per volume were acquired before contrast injection (field of view = 256×128, slice thickness = 5–10mm). Subsequently, an intravenous bolus injection (0.1 mmol/kg, 2ml/sec) of Gadolinium dimeglumine (Gd-DTPA) was administered. Image volumes were acquired every 30 seconds for 20 minutes.

Image Analysis

Relative enhancement images were fitted pixel-by pixel with a double exponential equation (equation1) using a non-linear iterative Chi square minimization technique based on the marquadt algorithm.

$$\Delta\text{Signal} = \text{Smax} * (1 - \exp(-\text{alpha} * \text{time})) * \exp(-\text{beta} * \text{time}) \quad (1)$$

Each fitted curve allowed the extraction of Smax (relative maximal enhancement constant), alpha (delivery rate constant) and beta (clearance rate constant) parameters. Negative values or values from the fit that never converged were not included for calculations of region of interest analysis. These parameters allowed the calculations of washin rate (Smax * alpha), washout rate (Smax * beta) along with area under the signal enhancement curve (AUC). With these parameters descriptors of perfusion/permeability were obtained. (16,17) For evaluation of AUC, three different integration times were chosen for calculation, AUC 60 (integration time from 0 to 60 seconds), AUC 90 (integration time from 0 to 90 seconds), and AUC t-max (integration time from 0 to when the muscle reference signaled peaked, t-max). Time to maximal muscle enhancement was calculated by setting the derivative of equation 1 to zero and solving for time. Otherwise this last value was used as the upper limit for calculating AUC

t-max. Representative patient image data is shown in Figure 2 for pre and post hyperthermia images and pseudo false color for washin, washout, and AUCt-max data.

From the fitted data, region of interest for tumor (including any necrosis) and muscle were manually drawn on each slice to form volumes of interest. Tumor region of interest included the entire tumor and potential necrosis and the muscle region of interest was drawn on muscle free of tumor in the field of view based on known normal anatomy. Median values were extracted from each volumes of interest. Washin, washout, AUC 60, AUC 90 and AUC t-max parameters were analyzed individually. This yielded five different parameters relating to perfusion/permeability. All imaging analyses were made with a custom made software running on MATLAB (The Mathworks, Inc., MA).

pH measurements

Extracellular pH measurements were made using needle microelectrodes ((Microelectrode, Inc., Londonderry, NH; Agulian, Hamden, CT), as previously described . Multiple measurements were made and averaged to obtain an overall estimate of the extracellular pH. Intracellular pH was determined by the frequency difference between the Pi and PCr resonances., from 31-P MRS spectra. MRS Spectra were acquired with a surface dual frequency coil array and triphenyl phosphite standards solutions were placed next to the tumor for pulse calibration. Pulse sequence protocol and data analysis methods have been previously reported in detail (14) (18)(2),

Treatment Endpoints

After treatment, dogs were reevaluated at 1, 2, 3, 5, 7, 9 and 12 months, and then at 3-month intervals. Reevaluation consisted of physical examination, tumor measurement, thoracic radiographs and assessment of regional lymph nodes. Tumors volumes were determine by direct physical measurements along 3 axis multiplied together with PI/6. Duration of local tumor control was defined as the time from date of the first hyperthermia treatment until local failure. Metastasis-free survival was defined as the time from date of the first hyperthermia treatment until metastasis or death, and overall survival was the time from date of the first hyperthermia treatment until death from any cause. Spread to regional lymph nodes was classified as positive for metastasis, as well as any spread to distant organs, such as the lung.

Statistical Analysis

Values of area under the curve were Log transformed due to the large range of calculated values, therefore throughout the paper AUC values reported will correspond to Log_{10}(AUC) values.

Each perfusion parameter was assessed for its predictive properties on metastasis free survival, time to local failure, and overall survival overall survival, before and after treatment, as well as their difference post - pre (Δ) treatment, using Cox proportional hazard ratio and Log Rank tests. The effect of the first hyperthermia treatment, as described by T50, T90, CEM43°C T50 and CEM43°C T90 along with administration time of hyperthermia on perfusion parameters obtained after the first hyperthermia was assessed using a Wilcoxon Rank sum test as well as a paired T test.

With one exception, multivariate analysis was not attempted for correlation with treatment outcome because of the limited number of subjects. Bivariate and multivariate analysis performed between perfusion related parameters and other clinical variables as well as the pH parameters to determine whether these were related to each other. Corrections for multiple comparisons were not made.

Results

Thirty-seven dogs (median age = 9.8 years, inter quartile range= 4.3 years) were evaluated with DCE-MRI before starting treatment. Seventeen of the dogs had a second DCE-MRI 24hr after the first thermoradiotherapy treatment. All subjects were planned to receive the second DCE-MRI study, but in 20 of these subjects, the data were either not obtained because of scheduling issues or because clean spectroscopic data could not be derived from the tissue for the second session which was required prior to the DCE-MRI per protocol design. The descriptive statistics of the sample characteristics are listed by thermal dose group in Table 1.

Thermal parameters

The population was balanced with respect to thermal dose group (low dose= 56.7%, and high dose= 43.3%). In the high thermal dose group, median temperature averaged T50 (median = 43.2°C; inter quartile range =1.9°C), T90 (median = 40.8°C; inter quartile range =0.7°C), CEM43°C T50 (median = 89.1 minutes; inter quartile range = 144.8 minutes) and CEM43°C T90 (median = 8.2 minutes; inter quartile range =6.4 minutes) and the total duration time of heating (median=214 minutes; inter quartile range=179.5 minutes). In the low thermal dose group, median temperature averaged T50 (median = 42.6°C; inter quartile range =1.7°C), T90 (median = 39.9°C; inter quartile range =0.6°C), CEM43°C T50 (median = 17.5 minutes; inter quartile range = 32.0 minutes) and CEM43°C T90 (median = 0.8 minutes; inter quartile range =0.6 minutes) and the total duration time of heating (median=103 minutes; inter quartile range=58 minutes).

The T50 and T90 values are descriptions of the frequency distribution of temperatures that are measured during treatment. The T50 is the median temperature and the T90 describes the temperature value that is exceeded by 90% of the measured values. This is sometimes referred to as the 10th percentile, but in the hyperthermia literature it has been traditionally referred to as the T90. CEM43° C is a conversion algorithm that converts any time-temperature history into an equivalent number of minutes at 43 °C. Details of this algorithm are published elsewhere.(19).

Predictors of clinical outcome

Cox proportional hazard ratio analyses demonstrated that several imaging-based parameters obtained prior to and after the first hyperthermia treatment were found to be significant in predicting metastasis free survival, time to local failure and overall survival along with total duration of heating (Table 2).

Local tumor control—AUC t-max (median = 5.1; inter quartile range = 0.65) measured before therapy was predictive of time to local failure (p=0.02); Figure 3a). There was no significant correlation between AUC t-max and tumor volume or grade in bivariate analysis (Table 3). However, because of competing risks of animals developing distant disease before reaching an endpoint for local tumor control, caution needs to be considered with respect to how to interpret this result.

Metastasis-free and overall survival—The median time to metastasis was 24 months and the 2 year overall survival rate was 0.36. This included animals that died and at necroscopy metastasis were found. Pre-treatment parameters that were found to be significant predictors of metastasis-free survival and overall survival included tumor grade ($p<=0.01$, 70%; intermediate/high=30%), volume ($p<0.05$, median 18.8 cm^3; inter quartile range of 55.7 cm^3) and washout ($p<=0.02$; median = 4.24; inter quartile range = 2.72, shown in Figure 3b). Better prognosis was associated with lower grade, smaller volume, and higher washout rate. The predictability of extracellular pH parameters (obtained using microelectrodes) from Lora-

Michiels et. al. are shown for comparison, since these measurements were taken on the same subjects (Table 2). (14)

AUC t-max, AUC 60, AUC 90 and washin parameter (Figure 3C) obtained 24hr following the first hyperthermia treatment were also significantly correlated with outcome. In all cases, higher values were associated with improved prognosis. These data suggest that improvements in perfusion and perhaps oxygenation after hyperthermia treatment are a good prognostic sign.

Multivariate analysis demonstrated that pre treatment AUC t-max and washout were independent predictors of metastasis free survival and overall survival ($p<0.05$, Table 3). In contrast, bivariate analysis demonstrated that AUC t-max obtained post treatment was inversely related to tumor volume and tumor grade. Small and/or low-grade tumors had higher AUC t-max values ($p<0.05$; Table 3). Washout values and AUC values obtained after treatment also were negatively correlated with tumor volume in bivariate analysis ($p<0.05$; Table 3).

Duration of Hyperthermia

The total duration of hyperthermia was found to be prognostically important in our previous report. (3) In this subset analysis, duration of heating remained an independent predictor of metastasis free survival and overall survival with hazard ratios of 1.28 and 1.32 and p-values of 0.007 and 0.004, respectively (Table 2). In this current study, heating duration was correlated with tumor grade in a bivariate analysis ($p<0.05$; Table 3).

Relationship with pH

Relationships between the MRI parameters measured here with pH parameters reported in our previous paper(14) are shown in Table 4. Bivariate analysis demonstrated that post hyperthermia washout values were negatively correlated with pre-treatment intracellular pH ($p<0.05$; Table 4) and positively correlated with the difference posttreatment (post-pre) pHe ($p<0.05$; Table 4). Figure 3d depicts the relationship of post washout with the change of pHe demonstrating a positive relationship, consistent with the notion that improved perfusion after heating leads to more efficient clearance of acid from the tissue.

DISCUSSION

This study demonstrated that DCE-MRI- based parameters may be useful in predicting overall and metastasis free survival in canine patients with soft tissue sarcomas. The parameters from the signal enhancement curve allowed prediction of patient outcome regardless of being done prior to the first hyperthermia therapy or 24 hours after. To our knowledge, this is the first time that DCE-MRI parameters have been shown to be predictive of clinical outcome for patients with soft tissue sarcomas. However, the results are based on a small number of patients, so larger clinical trials with adequate statistical power are needed to verify this initial result.

Measurements taken prior to treatment

For data acquired prior to treatment, AUC t-max emerged as being related to local tumor control. This parameter integrates signal over time for the tumor, truncating it when the signal reaches a maximum value in the reference muscle tissue. Consequently, this parameter probably relates to both perfusion and permeability. Tumors with higher AUC t-max might be better perfused and therefore better oxygenated. In bivariate analysis, this parameter was not associated with either tumor volume or grade, suggesting that it is an independent predictor of local tumor control (Table 3).

Higher washout values obtained prior to treatment were associated with greater metastasis-free and overall survival. This parameter relates to the reabsorption and clearance of contrast agent

from the extravascular space. Thus, higher values maybe associated with a vasculature that is more efficient in transport. Factors that influence transport efficiency include vascular density, permeability and perfusion rate of the microvessels. (20–23).

In prior studies we demonstrated theoretically that adjustments in microvessel orientation can make quite dramatic differences in oxygen transport. (20,21) The same principle should apply in reverse for an MR contrast agent. Thus, the combination of vascular density and orientation of microvessels are likely to contribute significantly to the differences in washout between different tumors.

Vascular permeability is related to the size of the solute, the concentration gradient across the microvessel wall and the physical characteristics of the vascular wall; due to the presence of large endothelial cell gaps and lack of basement membrane leading to increased permeability. (24,25) For large solutes, such as proteins, transport is strongly governed by convection generated by the pressure gradient across the vascular wall. With the presence of elevated tumor interstitial fluid pressure, these gradients are negligible. (24,25)

However, small molecules also undergo diffusive transport, so the influence of convection on the transport of a small molecule such as a chelated Gd contrast agent is negligible. Consequently, the Gd would likely be reabsorbed into the vasculature down its own concentration gradient once the kidneys clear the Gd from the general circulation. (24,25)

It is difficult to know why animals with tumors with better transport characteristics would have longer metastasis-free and overall survival. It may be reflective of a more differentiated state, but washout was not significantly associated with either tumor size or grade, suggesting that it could be independently predictive of outcome (Table 3).Current studies by our group are investigating interrelationships between physiologic/metabolic and genomic parameters, as compared with DCE/MRI. From this we may decipher more insight into this observation.

Measurements taken after the first heat treatment

It was surprising to find that DCE-MRI values obtained after the first hyperthermia treatment were also associated with outcome. Increases in AUC and washin after the first heat treatment were associated with prolonged metastasis free and overall survival (Table 3).This may relate back to the maturity of the vasculature. AUC t-max (along with other parameters) for the post treatment study were correlated with tumor volume and grade, suggesting that they may not be independent predictors of outcome. It is known that hyperthermia causes changes in permeability/perfusion but the distribution and amount may be dependent on the tumor volume/aggressiveness. Tumors with more mature vasculature may be able to respond more dynamically to thermal stress and therefore more readily increase perfusion in response to thermal stress. Presumably, tumors with more mature vasculature might be less likely to metastasize for a variety of reasons. They may be less hypoxic, which would tend to reduce upregulation of transcription factors that influence metastatic propensity, such as hypoxia inducible factor −1. (26).

DCE MRI as a clinical predictor

Only a few studies have been published describing the prognostic properties of DCE-MRI for clinical efficacy; studies involving gliomas, head & neck, breast, lung and cervical cancers have been reported (Appendix Supplemental Table 1).However, to our knowledge, clinical studies involving prediction of outcome for soft-tissue sarcomas using DCE-MRI have not been reported.

AUCt-max was the only perfusion parameter to predict local failure in our study (Table 2).Similar results have been reported by Mayr *et al.* in patients with cervical carcinomas at

early stages of radiation therapy using relative signal intensity parameters (Supplemental Table 1). (27,28)

Two studies have evaluated DCE-MRI parameters after treatment. Decreased tumor perfusion, at the end of a course of fractionated radiotherapy assessed by signal intensity perfusion indexes (Initial slope, Tmax) was related to low rates of local recurrence in patients in head and neck cancer. (29) Decreased perfusion indexes using the two compartment model, K^{trans} and Ve, had more than 65% tumor volume reduction after multimodality therapy in patients with breast cancer. (30) Similar to the head and neck trial these results are not surprising given they were obtained following therapy.

Although studies performed at the end of primary therapy are of interest scientifically, as they suggest that therapy eventually leads to reduction in perfusion, such information would have little impact on therapeutic choices. A more desirable approach is to predict likelihood of local control prior to/or during the early phases of treatment because such measurements could be used to alter the course of treatment and potentially lead to increased treatment efficacy.

Metastasis and Overall survival

Our results demonstrate that longer metastasis free survival and increased overall survival occurred in dogs with highly perfused tumors before hyperthermia treatment measured by increased washout rate and after treatment with increased washin rate, AUC: 60, 90 & t-max). Only one other study has been published that relates to these endpoints. An increased incidence of metastasis (and poorer survival) was observed in patients with Ewing's sarcomas displaying high percentage of necrosis. (31) The percentage of necrosis was obtained by calculating non-enhanced tumor regions from pre and post contrast enhanced images. Although this study did not specifically use dynamic MR parameters, lack of contrast agent is due to a lack of delivery, i.e. perfusion.

Thermal dose and changes in DCE-MRI parameters

Our patients were part of a large thermoradiotherapy clinical trial that tested effects of high vs. low thermal dose in dogs with spontaneous soft tissue sarcomas. (3) We reported that increased cumulative thermal dose was related to increased time to local failure. One potential mechanism underlying the improvement in local tumor control might be increased oxygenation, resulting from increased perfusion. We did not find an association between higher thermal dose and increased DCE-MRI parameters in this study, however. (Table 4).It may be that patient related parameters, such as the maturity of the vasculature or rates of tumor cell killing after the first thermoradiotherapy session had more of an influence on perfusion changes than thermal dose itself. Additionally, we did not measure changes in oxygenation of these tumors, so we cannot conclude whether the changes in DCE-MRI parameters were associated directly with improvements in tumor oxygenation. Studies of this type are ongoing now in our group.

Our prior analysis also showed that duration of heating time, independent of thermal dose, was related to metastasis free and overall survival. This recapitulates what we saw in the larger cohort of animals in this study. (3) A reasonable assumption might be that duration of heating would be related to perfusion in some way. For example the time required to reach the pre-determined thermal dose would be shorter for more poorly perfused tumors. In this subset analysis, we found that duration of heating was still important for overall and metastasis-free survival, but it was not related to any of the DCE/MRI parameters. There was a correlation between duration of heating and tumor grade. Higher grade tumors tended to take longer to adequately heat. This may have to do with a greater propensity for pre-existing necrosis in high grade tumors. Such tumors may develop power limiting hot spots in necrotic areas, which could

lead to the need to prolong heating times to get the rest of the tumor exposed to the prescribed thermal dose.

Using the same animals in this study, we recently reported that low extracellular pH (pHe) is associated with increased likelihood for tumor metastasis and shortened overall survival. (14) The acidic environment within tumors is thought to exist because of metabolic aberrations leading to propensity for anaerobic metabolism (e.g. the Warburg effect) and/or induction of anaerobic metabolism as a result of hypoxia (e.g. the Pasteur effect). However, the degree of acidosis will also be influenced by how efficiently the lactate is removed from the tissue by perfusion. In this study there was no relationship between DCE-MRI parameters obtained prior to treatment and pH, but an increase in washout was associated with an increase in pH. This is consistent with washout being indicative of a more efficient vascular system for waste removal. The inverse relationship between intracellular pH and washout is more difficult to explain. Generally, intracellular pH is tightly regulated by a variety of proton pumps that move lactate and hydrogen ions out of the cell to maintain a neutral intracellular pH. (32) It is difficult to reconcile how intracellular pH could have any influence upon changes in DCE-MRI parameters after hyperthermia treatment. This may be a spurious observation.

DCE-MRI analysis methods

There are two main models that have been used to derive physiologically-based parameters from dynamic images. The first is a two compartment model that includes the transfer coefficient between the intravascular and extravascular compartments (K^{trans}), the extracellular volume fraction and vascular volume fraction. (33,34) The second model is an empirical fit of the signal enhancement data of a pixel or region of interest. An area under the curve (AUC) can be calculated with this empirical fit. AUC calculations and the fitted values of the empirical equation can then be used to evaluate the dynamic data and referenced to normal tissue, such as muscle. (17,29,35–38) This second technique has the advantage of not requiring an arterial input function (arterial concentration-time curve of the contrast agent) for analysis.

All of these methods attempt to ascertain the meaning of the dynamic signal from DCE-MRI into physiologically tangible properties, i.e. tumor perfusion and vascular permeability. Several prior reports have shown correlations between DCE-MRI parameters and treatment outcome. (27,29,31,39–41)

In this study we used the second method, fitting the signal enhancement curve to an empirical equation. From this analysis, several DCE/MRI parameters were associated with treatment outcome in this study. In all cases, parameters that were associated with better overall perfusion indicated a better outcome. Being able to predict overall treatment outcome prior to, or shortly after treatment is initiated, potentially allows for treatment modification which may improve overall efficacy.

Limitations of the post-treatment data

Although the protocol called for scans to be taken prior to and 24h after the first hyperthermia treatment, only 17 of the original 37 animals actually had data at this second time point. There were multiple reasons for lack of data, but the two main ones related to lack of good data fits on the second session or scheduling conflicts. The scans were obtained on a human scanner and there were times when we were unable to schedule the canine patients for the second scan. We might have been able to avoid the poor data fitting on the second scan, had we been able to analyze the results immediately after the scan was done. Unfortunately, this was not possible at the time that these studies were done. In fact, we did not know about the problem until years later, when the data were post analyzed. We have encountered similar problems previously in human (18) studies. This points to the need for more rapid evaluation of study related

parameters, so that additional measurements could be made, thereby improving the data acquisition for studies that require multiple time points.

Canine sarcomas as models for human cancer

The canine sarcoma is an ideal model for human solid tumors in many respects. These advantages have been reviewed in detail, but are briefly summarized here. The natural history of canine sarcomas is very similar to that of humans (42). They are locally invasive and a proportion of them metastasize, making the achievement of local control challenging. For the purposes of hyperthermia studies, they are of the same size range as human tumors, making them amenable to heating, using the same heating technologies that are used in humans. There are many advantages of the canine tumor model in general. The patients are outbred and they are typically older and therefore have concomitant diseases like human patients do. They are immune competent, yet their tumors are only weakly antigenic, similar to humans (42). We have utilized this model extensively over the last 25 years.

Conclusion

Although the number of tumors imaged were limited, the results of this study suggest that DCE-MRI perfusion parameters are associated with various indicators of prognosis. Since delivery of nutrients (oxygen) and removal of waste (lactate) are dependent on perfusion, imbalances in delivery of nutrients and waste removal may contribute to aggressiveness of soft tissue sarcomas.

Supplementary Material

Refer to Web version on PubMed Central for supplementary material.

Acknowledgments

Supported by a NIH Grant PO1CA42745 from the Department of Health and Human Services

References

1. Datta NR, Bose AK, Kapoor HK, Gupta S. Head and neck cancers: results of thermoradiotherapy versus radiotherapy. Int J Hyperthermia 1990;6:479–486. [PubMed: 2198311]
2. Overgaard J, Gonzalez Gonzalez D, Hulshof MC, et al. Randomised trial of hyperthermia as adjuvant to radiotherapy for recurrent or metastatic malignant melanoma European Society for Hyperthermic Oncology. Lancet 1995;345:540–543. [PubMed: 7776772]
3. Thrall DE, LaRue SM, Yu D, et al. Thermal dose is related to duration of local control in canine sarcomas treated with thermoradiotherapy. Clin Cancer Res 2005;11:5206–5214. [PubMed: 16033838]
4. Valdagni, R.; Amichetti, M. Report of long-term follow-up in a randomized trial comparing radiation therapy and radiation therapy plus hyperthermia to metastatic lymph nodes in stage IV head and neck patients; Int J Radiat Oncol Biol Phys. 1994. p. 163-169.
5. van der Zee J, Gonzalez Gonzalez D, van Rhoon GC, van Dijk JD, van Putten WL, Hart AA. Dutch Deep Hyperthermia Group. Comparison of radiotherapy alone with radiotherapy plus hyperthermia in locally advanced pelvic tumours: a prospective, randomised, multicentre trial. Lancet 2000;355:1119–1125. [PubMed: 10791373]
6. Jones EL, Oleson JR, Prosnitz LR, et al. Randomized trial of hyperthermia and radiation for superficial tumors. J Clin Oncol 2005;23:3079–3085. [PubMed: 15860867]
7. Song CW. Effect of local hyperthermia on blood flow and microenvironment: a review. Cancer Res 1984;44:4721s–4730s. [PubMed: 6467226]
8. Vujaskovic Z, Song CW. Physiological mechanisms underlying heat-induced radiosensitization. Int J Hyperthermia 2004;20:163–174. [PubMed: 15195511]

9. Vujaskovic Z, Poulson JM, Gaskin AA, et al. Temperature-dependent changes in physiologic parameters of spontaneous canine soft tissue sarcomas after combined radiotherapy and hyperthermia treatment. Int J Radiat Oncol Biol Phys 2000;46:179–185. [PubMed: 10656391]
10. Thrall DE, Larue SM, Pruitt AF, Case B, Dewhirst MW. Changes in tumour oxygenation during fractionated hyperthermia and radiation therapy in spontaneous canine sarcomas. Int J Hyperthermia 2006;22:365–373. [PubMed: 16891239]
11. Milligan AJ, Panjehpour M. Canine normal and tumor tissue estimated blood flow during fractionated hyperthermia. Int J Radiat Oncol Biol Phys 1985;11:1679–1684. [PubMed: 3928546]
12. Brizel DM, Scully SP, Harrelson JM, et al. Radiation therapy and hyperthermia improve the oxygenation of human soft tissue sarcomas. Cancer Res 1996;56:5347–5350. [PubMed: 8968082]
13. Jones EL, Prosnitz LR, Dewhirst MW, et al. Thermochemoradiotherapy improves oxygenation in locally advanced breast cancer. Clin Cancer Res 2004;10:4287–4293. [PubMed: 15240513]
14. Lora-Michiels M, Yu D, Sanders L, et al. Extracellular pH and P-31 magnetic resonance spectroscopic variables are related to outcome in canine soft tissue sarcomas treated with thermoradiotherapy. Clin Cancer Res 2006;12:5733–5740. [PubMed: 17020978]
15. Bostock DE, Dye MT. Prognosis after surgical excision of canine fibrous connective tissue sarcomas. Vet Pathol 1980;17:581–588. [PubMed: 7404969]
16. Belfi CA, Paul CR, Shan S, Ngo FQ. Comparison of the effects of hydralazine on tumor and normal tissue blood perfusion by MRI. Int J Radiat Oncol Biol Phys 1994;29:473–479. [PubMed: 8005802]
17. Evelhoch JL. Key factors in the acquisition of contrast kinetic data for oncology. J Magn Reson Imaging 1999;10:254–259. [PubMed: 10508284]
18. Dewhirst MW, Poulson JM, Yu D, et al. Relation between pO2, 31P magnetic resonance spectroscopy parameters and treatment outcome in patients with high-grade soft tissue sarcomas treated with thermoradiotherapy. Int J Radiat Oncol Biol Phys 2005;61:480–491. [PubMed: 15667971]
19. Dewhirst MW, Viglianti BL, Lora-Michiels M, Hanson M, Hoopes PJ. Basic principles of thermal dosimetry and thermal thresholds for tissue damage from hyperthermia. Int J Hyperthermia 2003;19:267–294. [PubMed: 12745972]
20. Secomb TW, Hsu R, Braun RD, Ross JR, Gross JF, Dewhirst MW. Theoretical simulation of oxygen transport to tumors by three-dimensional networks of microvessels. Adv Exp Med Biol 1998;454:629–634. [PubMed: 9889943]
21. Secomb TW, Hsu R, Dewhirst MW, Klitzman B, Gross JF. Analysis of oxygen transport to tumor tissue by microvascular networks. Int J Radiat Oncol Biol Phys 1993;25:481–489. [PubMed: 8436527]
22. Secomb TW, Hsu R, Ong ET, Gross JF, Dewhirst MW. Analysis of the effects of oxygen supply and demand on hypoxic fraction in tumors. Acta Oncol 1995;34:313–316. [PubMed: 7779415]
23. Secomb TW, Hsu R, Park EY, Dewhirst MW. Green's function methods for analysis of oxygen delivery to tissue by microvascular networks. Ann Biomed Eng 2004;32:1519–1529. [PubMed: 15636112]
24. Jain RK. Physiological barriers to delivery of monoclonal antibodies and other macromolecules in tumors. Cancer Res 1990;50:814s–819s. [PubMed: 2404582]
25. Jain RK. Haemodynamic and transport barriers to the treatment of solid tumours. Int J Radiat Biol 1991;60:85–100. [PubMed: 1678003]
26. Semenza GL. Targeting HIF-1 for cancer therapy. Nat Rev Cancer 2003;3:721–732. [PubMed: 13130303]
27. Mayr NA, Yuh WT, Arnholt JC, et al. Pixel analysis of MR perfusion imaging in predicting radiation therapy outcome in cervical cancer. J Magn Reson Imaging 2000;12:1027–1033. [PubMed: 11105046]
28. Mayr NA, Yuh WT, Magnotta VA, et al. Tumor perfusion studies using fast magnetic resonance imaging technique in advanced cervical cancer: a new noninvasive predictive assay. Int J Radiat Oncol Biol Phys 1996;36:623–633. [PubMed: 8948347]
29. Hoskin PJ, Saunders MI, Goodchild K, Powell ME, Taylor NJ, Baddeley H. Dynamic contrast enhanced magnetic resonance scanning as a predictor of response to accelerated radiotherapy for advanced head and neck cancer. The British journal of radiology 1999;72:1093–1098. [PubMed: 10700827]

30. Pickles MD, Lowry M, Manton DJ, Gibbs P, Turnbull LW. Role of dynamic contrast enhanced MRI in monitoring early response of locally advanced breast cancer to neoadjuvant chemotherapy. Breast Cancer Res Treat 2005;91:1–10. [PubMed: 15868426]

31. Dunst J, Ahrens S, Paulussen M, Burdach S, Jurgens H. Prognostic impact of tumor perfusion in MR-imaging studies in Ewing tumors. Strahlenther Onkol 2001;177:153–159. [PubMed: 11285773]

32. Madshus IH. Regulation of intracellular pH in eukaryotic cells. Biochem J 1988;250:1–8. [PubMed: 2965576]

33. Toftss PS, Brix G, Buckley DL, et al. Estimating kinetic parameters from dynamic contrast-enhanced T(1)-weighted MRI of a diffusable tracer: standardized quantities and symbols. J Magn Reson Imaging 1999;10:223–232. [PubMed: 10508281]

34. Leach MO, Brindle KM, Evelhoch JL, et al. The assessment of antiangiogenic and antivascular therapies in early-stage clinical trials using magnetic resonance imaging: issues and recommendations. Br J Cancer 2005;92:1599–1610. [PubMed: 15870830]

35. Lyng H, Vorren AO, Sundfor K, et al. Assessment of tumor oxygenation in human cervical carcinoma by use of dynamic Gd-DTPA-enhanced MR imaging. J Magn Reson Imaging 2001;14:750–756. [PubMed: 11747032]

36. Tuncbilek N, Karakas HM, Okten OO. Dynamic contrast enhanced MRI in the differential diagnosis of soft tissue tumors. Eur J Radiol 2005;53:500–505. [PubMed: 15741025]

37. Siegmann KC, Muller-Schimpfle M, Schick F, et al. MR imaging-detected breast lesions: histopathologic correlation of lesion characteristics and signal intensity data. AJR Am J Roentgenol 2002;178:1403–1409. [PubMed: 12034606]

38. Hawighorst H, Knapstein PG, Knopp MV, Vaupel P, van Kaick G. Cervical carcinoma: standard and pharmacokinetic analysis of time-intensity curves for assessment of tumor angiogenesis and patient survival. Magma 1999;8:55–62. [PubMed: 10383094]

39. Wong ET, Jackson EF, Hess KR, et al. Correlation between dynamic MRI and outcome in patients with malignant gliomas. Neurology 1998;50:777–781. [PubMed: 9521274]

40. Mayr NA, Taoka T, Yuh WT, et al. Magnetic resonance imaging in the assessment of radiation response in cervical cancer: regarding Hatano K et al. IJROBP 1999; 45:399–344. Int J Radiat Oncol Biol Phys 2000;48:910–912. [PubMed: 11183740]

41. Postema S, Pattynama PM, van Rijswijk CS, Trimbos JB. Cervical carcinoma: can dynamic contrast-enhanced MR imaging help predict tumor aggressiveness? Radiology 1999;210:217–220. [PubMed: 9885611]

42. Dewhirst, MW.; Thrall, D.; MacEwen, EG. Spontaneous pet animal cancers. In: Teicher, B., editor. Tumor models in cancer research. Totowa, NJ: Humana Press; 2002. p. 565-590.

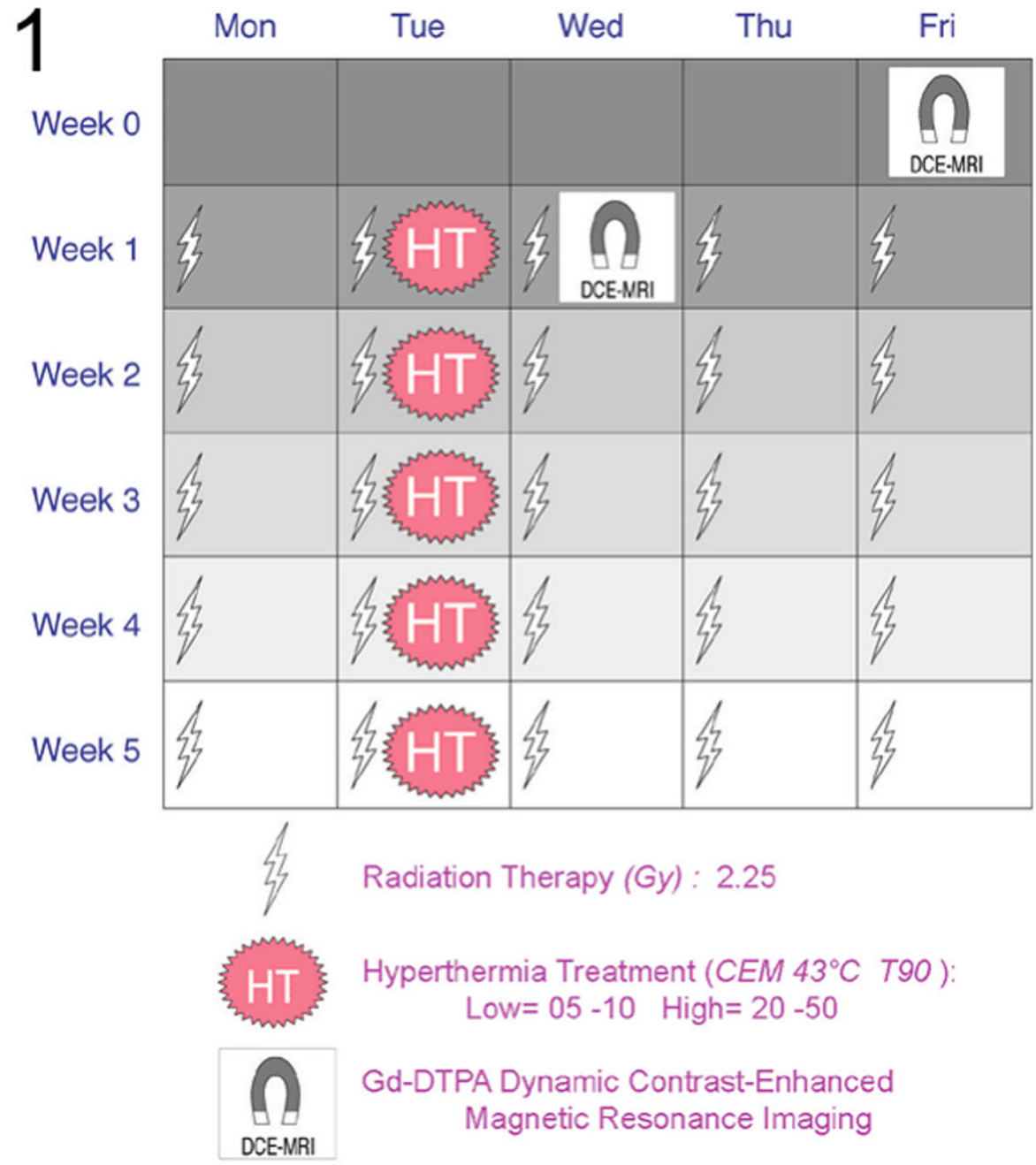

Figure 1.
graphical representation of the treatment and MRI acquisition schedule for this trial.

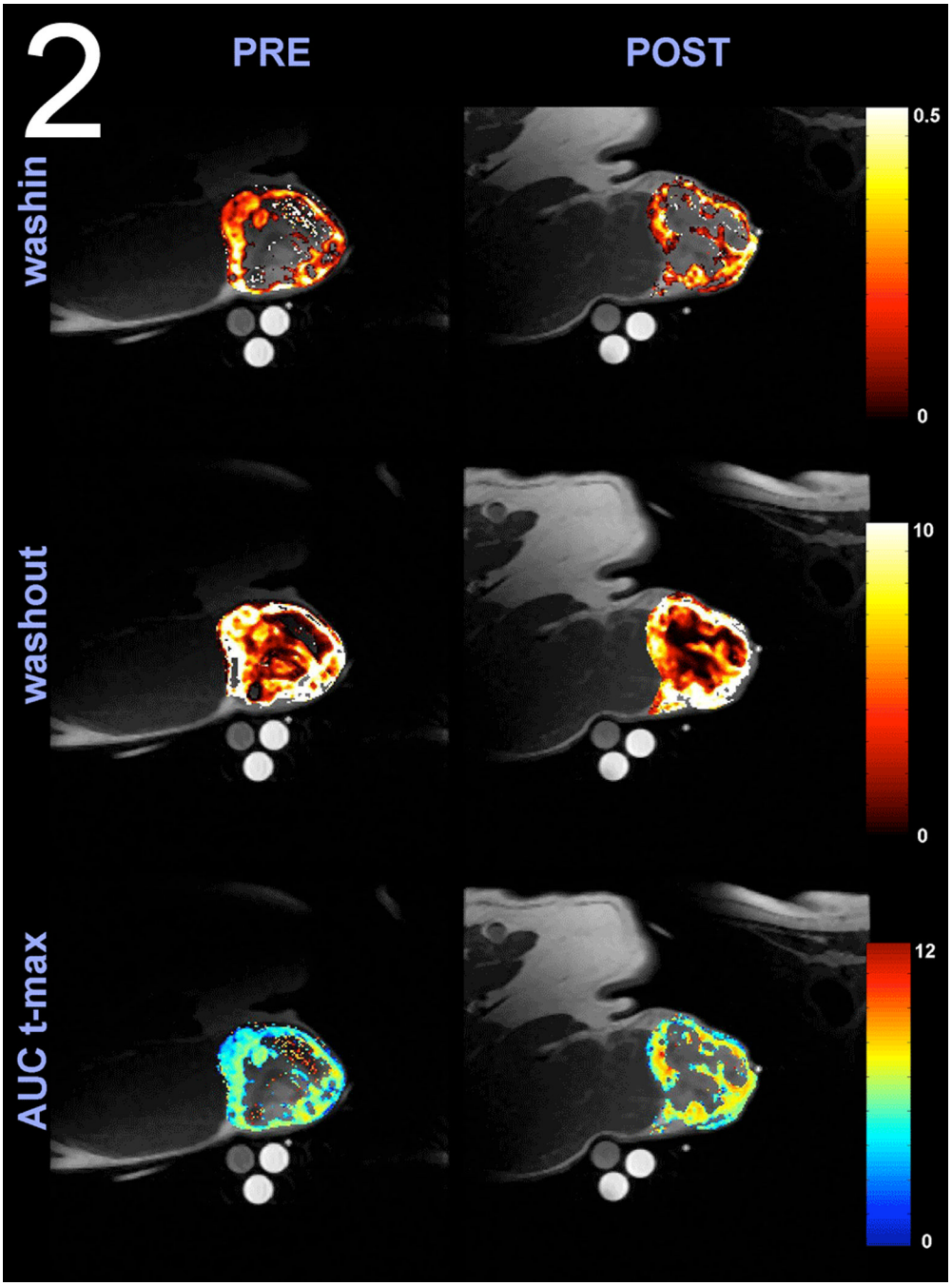

Figure 2.
Overlay of anatomical T1 images with washin, washout, and AUC t-max perfusion maps obtained from a canine patient with a hemangiopercytoma of the perineum using DCE-MRI. Note the heterogeneity in tumor perfusion and the increase in AUC t-max post 24 hour post hyperthermia. AUC t-max is the Area Under the Curve of the dynamic signal enhancement between 0 and the time of maximal muscle enhancement. AUC values are expressed in Log_{10}.

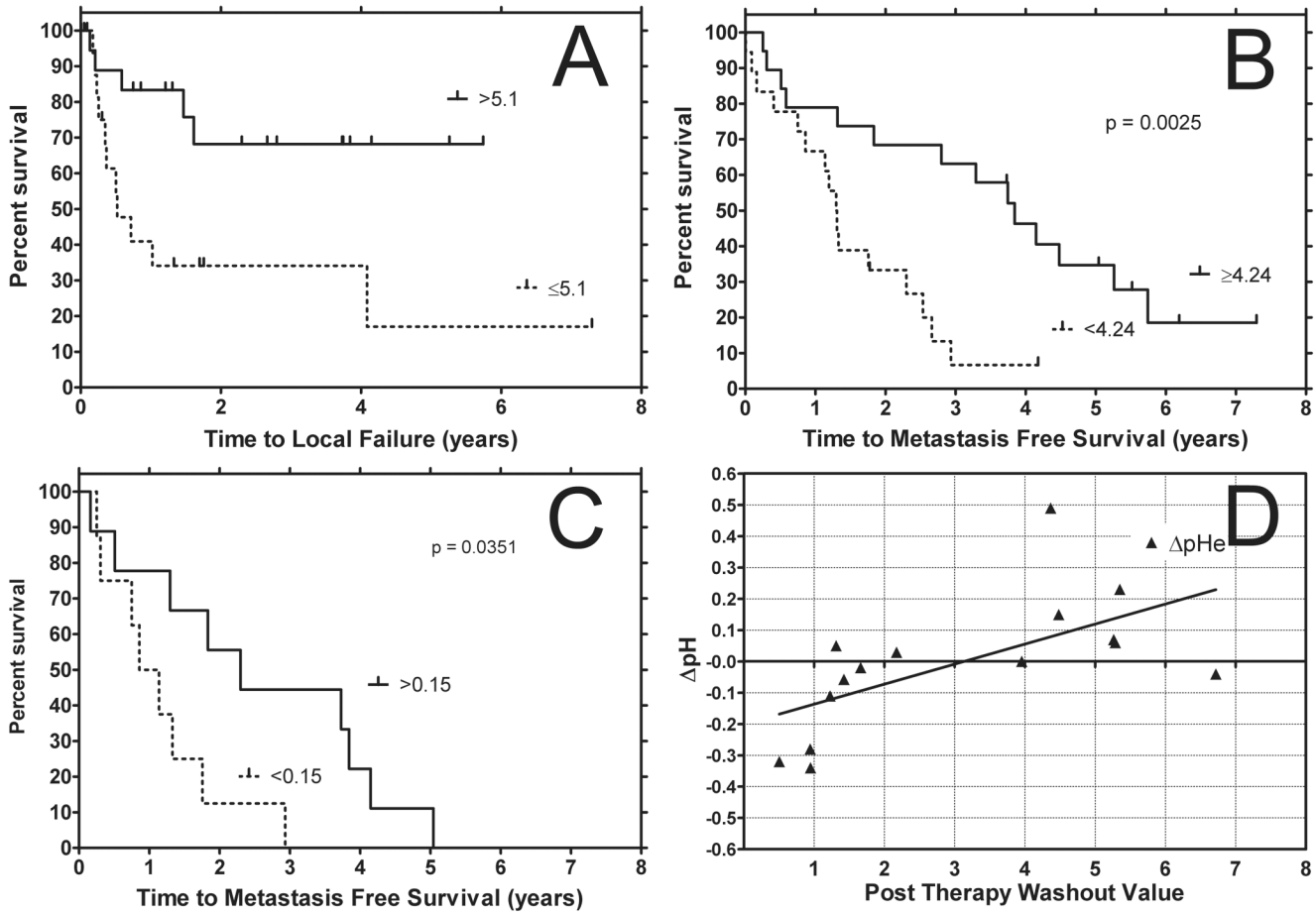

Figure 3.

(a) Kaplan Meier plot depicting time to local failure for tumors with AUC t-max values (expressed in Log10 form) above and below their cut point values. (cut point = Interquartile range/2). Kaplan Meier plot depicting metastasis free survival for tumors with washout values above and below their cut point values (cut point = Interquartile range/2) before treatment (b) and washin 24 hours post hyperthermia with a similarly calculated cut point (c). Relationship of pHi-Pre and pHe@24hr - pHe-Pre versus washout measured with DCE-MRI (d). Interstitial pH prior to therapy shows a negative correlation with increasing post washout values. Changes in extracellular pH from therapy show a positive correlation with increase post washout values. This suggests that following therapy the ability to remove the contrast agent results is greater ability to also remove acid from the extracellular environment of tumors that are more acidic prior to therapy. This agrees with the assumption that hyperthermia improves perfusion and removal of the contrast agent is suggestive of this.

Table 1

Sample Characteristics by Thermal Dose Group. Descriptive statistics of the treated tumors separated by thermal dose groups. Histological types are expressed as a percent of the total population. FSA = Fibrosarcoma, HPC = Hemangiopericytoma, MYX = Myxosarcoma, NFS = Neurofibrosarcoma, SA = Sarcoma

Variable	Low Dose Mean (Std) or % N=21	High Dose Mean (Std) or % N=16	All Subjects Mean(Std) or % N=37
Age(years)	10.1(2.8)	10.1(3.1)	10.1(2.9)
Tumor Volume (cm^3)	48.6(69.0)	44.5(42.2)	46.8(58.2)
Low Tumor Grade	76.2%	62.5%	70.3%
High Tumor Grade	23.8%	37.5%	29.7%
FSA Histology Type	14.3%	25%	18.9%
HPC Histology Type	52.4%	50%	51.4%
MYX Histology Type is	9.5%	12.5%	10.8%
NFS Histology Type is	4.8%	6.3%	5.4%
SA Histology Type is	9.5%	0	5.4%
Other Histology Type	9.5%	6.2%	8.1%

Table 2

Statistical results, hazard analysis for Metastisis Free Survival, Time to Local Failure, and Overall Survival. Summary of Cox proportional hazard ratio analysis showing significant perfusion/permeability predictors of clinical outcome determined with signal based DCE-MRI. The pre washout rate was predictive for metastasis free survival and overall survival while AUC t-max was predictive in time to local failure. For the post image analysis all the AUC calculation and the washin rates were predictive of metastasis free survival and overall survival. The pre pHe, the difference in pHe between pre and post therapy, and heating duration were also predictive of metastasis free survival and overall survival. (overall survival = overall survival, MFS = metastasis free survival, TFL = tumor local failure, pHe = extracellular pH, pHi = interstitial pH)

	Parameter	I.C	MFS		TLF		OS	
			HR	p-value	HR	p-value	HR	p-value
PRE n=37	**Grade**	H vs. L	**1.63 (1.1–2.4)**	**0.010**	1.36 (0.8–2.3)	0.230	**1.65 (1.1–2.4)**	**0.008**
	Volume	27.9cc	**1.15 (1.0–1.3)**	**0.049**	1.05 (0.8–1.3)	0.620	**1.16 (1.0–1.3)**	**0.040**
	AUC 60	0.3	0.80 (0.6–1.1)	0.220	0.88 (0.6–1.4)	0.582	0.81 (0.6–1.2)	0.247
	AUC 90	0.3	0.80 (0.6–1.1)	0.209	0.87 (0.6 –1.4)	0.562	0.81 (0.6 1.1)	0.234
	AUC t-max	0.3	0.89 (0.7–1.1)	0.310	**0.66 (0.5–0.9)**	**0.020**	0.89 (0.7–1.1)	0.320
	Washin	0.1	0.89 (0.7–1.1)	0.331	0.86 (0.6–1.2)	0.381	0.89 (0.7–1.1)	0.338
	Washout	1.4	**0.68 (0.5–0.9)**	**0.015**	0.87 (0.6–1.3)	0.500	**0.67 (0.5–0.9)**	**0.012**
POST n=17	**AUC 60**	0.3	**0.44 (0.3–0.7)**	**0.001**	0.84 (0.5–1.5)	0.540	**0.49 (0.3–0.8)**	**0.001**
	AUC 90	0.3	**0.45 (0.3–0.7)**	**0.001**	0.85 (0.5–1.5)	0.550	**0.49 (0.3–0.8)**	**0.001**
	AUC t-max	0.4	**0.46 (0.3–0.8)**	**0.002**	0.65 (0.4–1.2)	0.170	**0.46 (0.3–0.8)**	**0.001**
	Washin	0.1	**0.55 (0.4–0.9)**	**0.004**	0.76 (0.5–1.3)	0.270	**0.53 (0.3–0.8)**	**0.002**
	Washout	1.7	0.82 (0.5–1.3)	0.414	1.16 (0.6–2.1)	0.65	0.82 (0.5–1.3)	0.402
PH	**pHi-Pre (n=30)**	H vs. L	0.54(0.2–1.3)	0.150	0.49(0.2–1.5)	0.199	0.58(0.3–1.3)	0.199
	pHi@24hr-pHi-Pre (n=15)	H vs. L	1.44(0.5–4.6)	0.538	7.70(0.9–66.2)	0.063	1.41(0.4–4.5)	0.565
	pHe-Pre (n=30)	H vs. L	**0.29(0.1–0.7)**	**0.005**	0.84(0.27–2.60)	0.767	**0.36(0.2–0.8)**	**0.013**
	pHe@24hr-pHe-Pre (n=24)	H vs. L	**2.87(1.1–7.6)**	**0.034**	1.59(0.5–5.5)	0.465	2.54(1.0–6.7)	0.061
HTmin	**Total Duration of Heat (min)**		**1.28(1.1–1.5)**	**0.007**	1.18(0.9–1.5)	0.149	**1.32(1.09–1.60)**	**0.004**

MFS = metastasis free survival , TLF = time to local failure, OS = overall survival

I.C = Incremental change (of respective unit)

HR = hazard ratio (confidence interval)

AUC 60 = area under the curve integrated up to 60 sec

AUC 90 = area under the curve integrated up to 90 sec
AUC t-max = area under the curve integrated up to time to muscle peak

Table 3

Summary of bivariate analysis showing the relationship between tumor volume and tumor grade with the significant perfusion/ permeability estimators obtained with Gd-DTPA DCE-MRI. All of the post MRI image parameters were found to correlate with tumor volume. AUC t-max and washin correlated with tumor grade. Therefore it is not possible to determine whether these parameters are independent predictors of outcome.

		Tumor Volume		Tumor Grade	
		Spearman	**p -value**	**Exact Rank sum test**	**T Test**
	AUC60	−0.239	0.155	0.256	0.3
	AUC90	−0.241	0.151	0.242	0.294
Pre	**AUC t-max**	−0.208	0.216	0.124	0.182
	Washin	−0.175	0.3	0.756	0.787
	Washout	−0.293	0.079	0.141	0.189
	AUC 60	**−0.500**	**0.041**	0.506	0.379
	AUC 90	**−0.515**	**0.035**	0.646	0.346
Post	**AUC t-max**	**−0.610**	**0.009**	**0.009**	**0.008**
	Washin	**−0.534**	**0.027**	**0.234**	**0.039**
	Washiout	**−0.586**	**0.014**	0.328	0.189
HT(min)	HT(min)	0.244	0.146	**0.033**	0.104

AUC 60 = area under the curve integrated up to 60 sec
AUC 90 = area under the curve integrated up to 90 sec
AUC t-max = area under the curve integrated up to time to muscle peak

Table 4

Summary analysis showing the relationship between the MRI parameters measured to pH parameters. pHi = interstitial pH and pHe = extracellular pH. Only the difference between pHe pre and post therapy was found correlate with post washout values. Bold and shaded cells were significant and bolded image parameters were the ones significant in predicting outcome as shown in Table 1

		pHi-Pre		pHi@24hr - pHi-Pre		pHe-Pre		pHe@24hr - pHe-Pre	
		Spearman	**p -value**	**Spearman**	**p -value**	**Spearman**	**p -value**	**Spearman**	**p -value**
Pre	AUC60	0.034	0.868	0.169	0.563	0.023	0.912	0.02	0.93
	AUC90	0.046	0.818	0.143	0.626	0.034	0.871	0.01	0.966
	AUC t-max	−0.163	0.417	0.037	0.899	0.099	0.63	0.098	0.665
	Washin	0.006	0.976	0.174	0.553	0.032	0.877	0.132	0.56
	Washout	0.027	0.894	−0.486	0.078	0.149	0.467	−0.014	0.95
Post	AUC 60	−0.118	0.676	−0.036	0.916	0.256	0.358	0.086	0.761
	AUC 90	−0.125	0.657	0.036	0.916	0.256	0.358	0.125	0.657
	AUC t-max	−0.236	0.398	0.036	0.916	0.225	0.42	0.254	0.362
	Washin	−0.236	0.398	0.173	0.612	0.32	0.245	0.293	0.29
	Washout	**−0.643**	**0.01**	0.182	0.593	−0.288	0.298	**0.736**	**0.002**
HT(min)	HT(min)	0.066	0.744	0.077	0.794	−0.204	0.317	−0.213	0.342

AUC 60 = area under the curve integrated up to 60 sec
AUC 90 = area under the curve integrated up to 90 sec
AUC t-max = area under the curve integrated up to time to muscle peak